31st Annual International Conference of the IEEE EMBS
Minneapolis, Minnesota, USA, September 2-6, 2009

Experimental Validation of an Optical System for Interrogation of Dermally-Implanted Microparticle Sensors

Ruiqi Long and Mike McShane, *Senior Member, IEEE*

Abstract— **Dermally-implanted microparticle sensors are being developed for on-demand monitoring of blood sugar levels. For these to be deployed *in vivo*, a matched opto-electronic system for delivery of excitation, collection and analysis of escaping fluorescent signal is needed. Previous studies predicted the characteristics of fluorescence from microparticle sensors to facilitate design of hardware system. Based on the results of simulations, we designed and constructed the optical part of this opto-electronic system. This study experimentally verified the simulation results and tested the capability of the designed optical system. Reliable skin phantoms sufficient for future dynamic tests were developed. Skin phantoms with different thicknesses were made and the optical properties of skin phantoms were determined with an integrating sphere system and Inverse Adding-Doubling method. Measurements of sensor emission spectrum through phantoms with different thicknesses were done with the designed optical system. Simulations for the experiment situation were performed. The experimental measurements agreed well with simulations in most cases. The results of hardware experiment and validation with skin phantoms provided us with critical information for future dynamic tests and animal experiments.**

I. Introduction

THE development of a noninvasive sensor for *in vivo* monitoring of glucose in interstitial fluid to facilitate patient control of diabetes mellitus is being pursued by hundreds of research groups worldwide. Various "minimally-invasive" biosensors have showed promise, particularly using fiber optic technology and highly-sensitive fluorescence approaches [1-5]. However, fiber-optic systems require invasion by the probe and have not proven to meet the stability or reliability requirements for long-term *in vivo* functionality. A potential solution for the probe interface is to detach the probe chemistry from the fiber tip, resulting in a completely implantable sensor retained in the tissue much like cosmetic dermal filling agents or tattoos [6-9]. A useful implantable device must be biocompatible, must not exhibit acute reagent consumption or degradation, and must provide means of communicating the sensor output to the physicians or patients.

Manuscript received April 7, 2009. This work was supported in part by the National Institutes of Health under grant R01 EB000739.

R. Long is with the Department of Biomedical Engineering, Texas A&M University, College Station, TX 77843 USA (e-mail: orangesay@tamu.edu).

M. McShane is with the Department of Biomedical Engineering, Texas A&M University, College Station, TX 77843 USA (phone: 979-845-7941; fax: 979-845-4450; e-mail: mcshane@tamu.edu).

We have recently reported several different fluorescent chemo-optical sensor systems that may meet the needs of implantable biochemical indicators, including those based on self-assembled hybrid microparticles [10-13]. *In vitro* results suggest that adequate sensitivity, reliability, and longevity may be achieved with these systems.

Given that these sensors can be developed to meet the requirements for *in vivo* use, it is envisioned that a bed of microspheres containing of sensing chemistry may be injected in the dermis to interact with the interstitial fluid to monitor blood sugar level or other biochemicals of interest. For these sensors to be deployed *in vivo*, a matched opto-electronic system for delivery of excitation, collection and analysis of escaping fluorescent signal is needed. It is therefore necessary to predict the characteristics of fluorescent signal from dermally-implanted microparticle sensors under *in vivo* conditions to facilitate design of this desired hardware system.

In previous work, 3D optical analysis software package with Monte Carlo ray-tracing capability (OptiCAD® 10.033) was used to simulate photon transport through skin and interaction with fluorescent implants to predict spectral and spatial distribution of fluorescence signal. Based on the results of simulations, a hardware system for delivery of excitation light and collection of fluorescent emission was designed and constructed.

The aim of this study is to experimentally verify the optical system that was designed based on the previous results of Monte Carlo simulation. This work is a transition between simulation work and future animal experiments.

II. Materials and Methods

A. Simulation System

The diagram of optical design was shown in Fig. 1. The optical system model (Fig. 2) simulated the optics in experiments. All the lens models were imported from lens catalogue of OptiCAD®. The simulation considers one excitation (540nm) and six emission wavelengths (570nm, 585nm, 620nm, 635nm, 645nm and 665nm). Emission spectrum used in simulations was emission spectrum collected when sensors were exposed in the air. In Fig. 2, Film 1 was used as a detector film to capture fluorescent emission photons which should be collected by detectors. We changed the distance between the last surface of lens e and the surface of skin model from 1.8mm~2.0mm to

estimate the displacement errors of samples that may be attributed to manually handling of samples during experiments.

A homogeneous skin model was created to mimic the skin layers that are above the region where microparticle sensors are intended to be introduced. Those layers included stratum corneum, epidermis, papillary dermis, upper blood plexus and reticular dermis, which are based on the eight-layer skin model used by Zeng, et al. [14]. A review of literature on skin optical properties was used to identify refractive index, absorption, scattering, and scattering anisotropy value of each layer of the eight-layer model [14-16]. The optical properties of the homogeneous skin model used in simulation were calculated as a weighted average by adding the products of the optical properties of eight-layer model and the corresponding volume factors [17].

Microparticle sensor patch was modeled as a cylindrical slab with 3mm in diameter and 20μm high to mimic the dimension of sensor sample we used in experiment. The absorption coefficient of sensors was calculated from the molar extinction coefficient ($11.16mm^{-1}$) of sensors fabricated containing platinum octaethylporphine (PtOEP) and rhodamine isothiocyanate (RITC) as indicator and reference dyes, respectively [18].

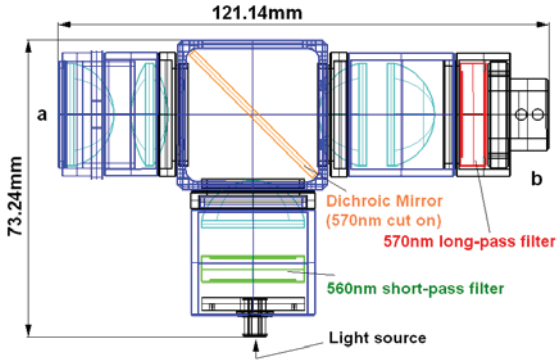

Fig. 1. Diagram of optical system design. Part a is for delivery of excitation light reflected by the dichroic mirror and focused on the skin or phantom; part b is for collection of fluorescent emission light and is connected to a spectrometer via a optical fiber to analyze spectrum of emssion light.

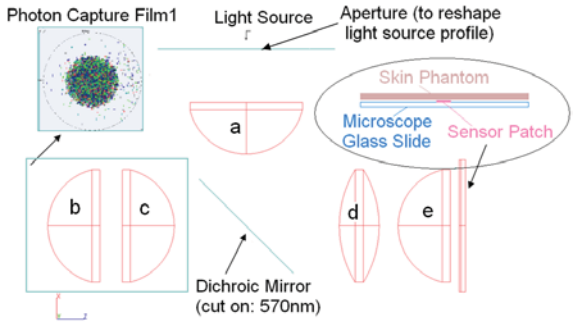

Fig. 2. Scheme of simulation system. A lens tube was positioned outside lens b and c to block the latterally reflected fluorescent emission photons. Emission profile of light source was shaped as a cone with solid angle 0.84 sr.

B. *Skin Phantoms*

Homogeneous skin phantoms were made to mimic the average optical properties of human skin. The main component was silicone elastomer base (SYLGARD® USA) mixed with curing agent at a ratio of 9:1 by weight. The refractive index of silicone (1.404 [19]) is similar to that of soft mammalian-tissue (1.33-1.50) [20]. We used cosmetic powder (Cream Powder, Deep Beige, Max Factor, UK) [19] to mimic the main absorption attributes over excitation and emission range of our sensors (500nm-700nm). Red ink (DESIGN Higgins®, SANFORD) was used as additional absorber to mimic the optical properties of oxygenated blood. The main scattering agent was Aluminum Oxide (Al_2O_3) powder (10μm 99.7 % metals basis, Sigma Aldrich®). We mixed 597.7mg Al_2O_3 powder, 12.66mg cosmetic powder, 1.67μL red ink, and 111.1μL curing agent per milliliter silicone base and stirred until homogeneously distributed, and then cured for at least 24 hours at room temperature. All the phantoms used in experiments were left at room temperature for at least a week before experiment. The thickness of phantoms ranged from 30μm to 1.8mm.

C. *Determination of Optical Properties of Skin Phantoms*

The absorption and scattering coefficients of skin phantoms were determined by integrating sphere (IS) systems (Fig. 3) and Inverse Adding-Doubling (IAD) software available on line [21]. We collected specta for total reflection and transmission of each sample with IS and a spectrometer (USB 4000, Ocean Optics, Inc.) coupled via 1mm core fiber at the detection port (port 2). Integration time was 1 second. The light source was Tungsten Halogen Light Source (LS-1, Ocean Optics, Inc.) collimated by a collimating lens (F220SMA, Thorlabs, Inc.). For measurements of total reflection (sum of diffuse and specular reflections), the light source was placed at the entrance port (port 1) and the collimated illumination beam formed a spot size around 6mm in diameter on the sample. All the samples were sandwiched between two 1mm-thick microscope glass slides and placed at sample port (port 3) during all measurements. Total reflectance was calibrated using 10% and 50% reflectance standards (SRS-10-010, SRS-50-010, Labsphere®, North Sutton, New Hamsphire). For total transmission measurement, the light source was placed in front of the sample port illuminating sample by a spot with the same size as that in reflection measurement. The total transmittance was normalized to the incident power. Optical properties were calculated with IAD software (v 3.5.1, 23 May 2008). The algorithm of IAD is iterating adding doubling solution of the radiative transport equation until the calculated results of the reflectance and transmittance matched the measured ones [22]. The scattering anisotropy value (g) was assumed and set 0.77 before running the program and only total reflectance and transmittance were used for IAD calculation.

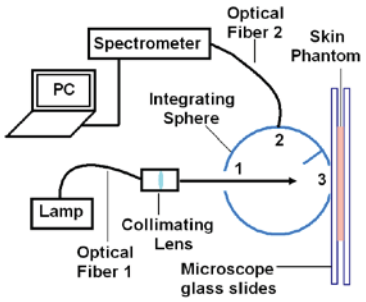

Fig. 3. Scheme of integration sphere system to measure optical properties of skin phantoms

D. *Experiment System*

The scheme of experiment was shown in Fig. 4. A sensor sample was attached on a microscope glass slide by a double-sided sticky tape. Skin phantoms with various thicknesses covered the sensor sample. Excitation light from a green LED (λ_{peak}=530nm, LS-530, Sandhouse, Dunedin, Florida, USA) was focused on the skin phantoms. The integration time of the spectrometer was 25ms for every measurement.

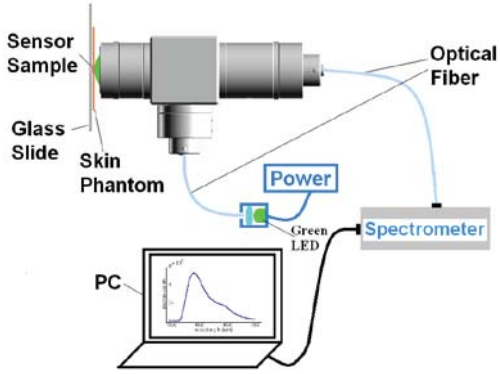

Fig. 4. Scheme of experiment system.

III. Results and Discussion

A. *Optical Properties of Skin Phantoms*

The absorption and scattering coefficients of phantoms were given in Fig. 5. In Fig. 5(a), the measured absorption coefficients of phantoms matched well with the absorption coefficients of human skin used in simulations for skin model, especially in the longer wavelength range (570nm – 670nm). In Fig. 5(b), scattering coefficients from the main scattering agent Al_2O_3 powder were predicted by Mie scattering calculations [23]. Al_2O_3 powder was assumed to be spheres with diameter in 10μm in Mie scattering calculations. Though the variances of measured scattering coefficients were around 30%, there were still a good agreement of the measured values of phantoms, values of skin, and the predicted values from Mie scattering theory.

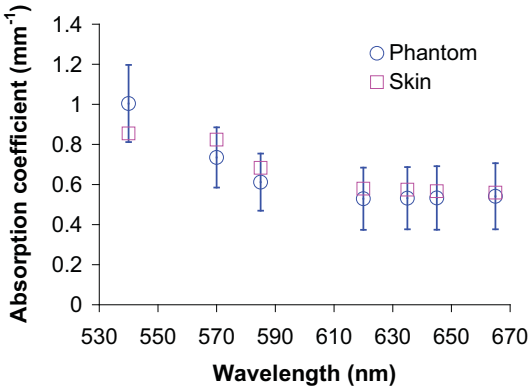

Fig. 5(a): Blue circles are calculated absorption coefficients (μ_a) of skin phantoms. Pink squares are μ_a of skin used in simulations. Error bars: one standard deviation.

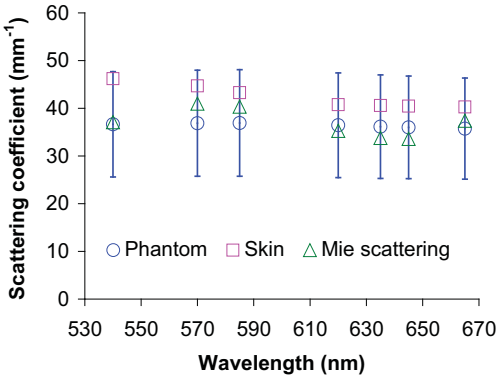

Fig. 5(b): Blue circles are calculated scattering coefficients (μ_s) of skin phantoms. Pink squares are μ_s of skin used in simulation. Green triangles are μ_s predicted by Mie scattering calculation Error bars: one standard deviation.

B. *Comparison of Experimental and Simulation Results*

In experiments, the emission of sensor sample through a phantom was collected by the optical system and analyzed by the spectrometer. In simulations, six discrete wavelengths were simulated for the optical system and skin models with various thicknesses. In Fig. 6, specta of sensor emission through a phantom with thickness 451μm was compared with the simulation results. The distance between the last surface of last lens and the surface of skin model was changed from 1.8mm to 2.0mm to estimate the discrepancy of sample positions during experiments. Though the variance due to changed skin-lens distance was large, the average spectrum still showed a good agreement with experimental results. The attenuation ratio was the ratio of emission intensity of sensor sample through a phantom to that without a phantom covered. The attenuation ratio at 585nm and 645nm versus thickness of phantoms were given and compared with simulation results in Fig. 7. Phantoms were made from three different batches (batch A, B and C) with the same recipe. The results of experiment and simulation agreed well in most cases.

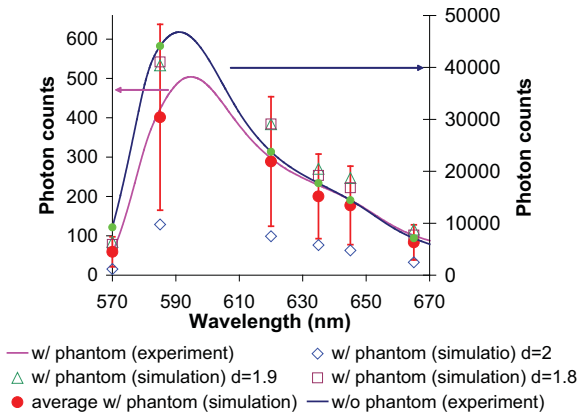

Fig. 6. Comparison of simulated and experimental emission spectra. Green circles are the six wavelengths selected for simulations. Error bars: one standard deviation of three simulations for different distances. In legend, the "d=2, 1.8, 1.9" indicated the skin-lens distance in simulations was 2mm, 1.8mm and 1.9mm.

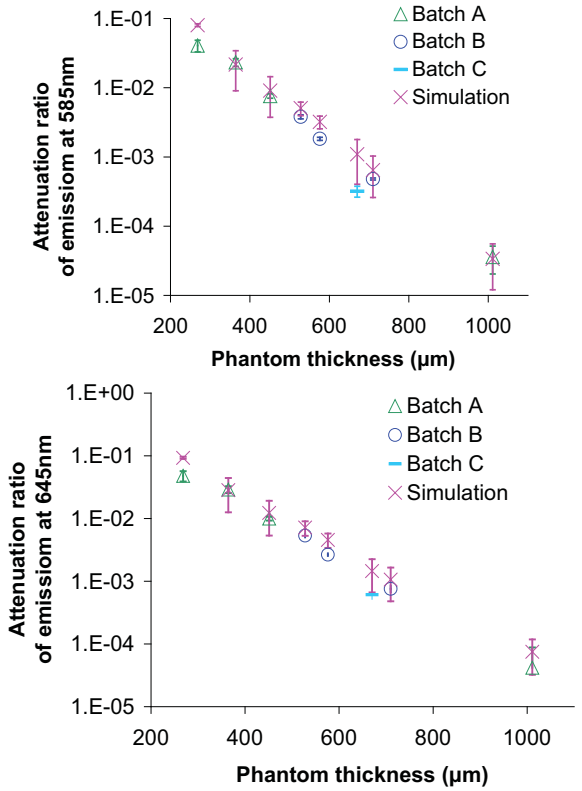

Fig. 7. Comparison of attenuation ratio at 585nm (top) and 645nm (bottom). Error bars indicate one standard deviation. Some error bars were too small to be plotted.

IV. Conclusion

The silicone-based skin phantoms mimic the optical properties of human skin, and have the advantages of stability and feasibility to produce multi-layered structures. The experimental validations showed an excellent agreement with simulation, proving that the optical hardware meets expectations for *in vivo* analysis of implants. The phantoms and optical system will be used for extensive *in vitro* sensor validation prior to use in animal experiments.

Acknowledgment

The authors acknowledge NIH (grant R01 EB000739), Dr. Kenith Meissner and technical support from Mr. Edward Sklar (OptiCAD®).

References

[1]J. S. Schultz and G. Sims, "Affinity sensors for individual metabolites," Biotechnol Bioeng Symp, pp. 65-71, 1979.

[2]W. Trettnak, M. J. P. Leiner, and O. S. Wolfbeis, "Fibre-optic glucose sensor with a pH optrode as the transducer," Biosensors, vol. 4, p. 15, 1989.

[3]M. C. Moreno-Bondi, O. S. Wolfbeis, M. J. Leiner, and B. P. Schaffar, "Oxygen optrode for use in a fiber-optic glucose biosensor," Anal Chem, vol. 62, pp. 2377-80, Nov 1 1990.

[4]O. S. Wolfbeis, "Fiber optic biosensing based on molecular recognition," Sensors and Actuators, B: Chemical, vol. B5, p. 1, 1991.

[5]R. Ballerstadt and J. S. Schultz, "A fluorescence affinity hollow fiber sensor for continuous transdermal glucose monitoring," Anal Chem, vol. 72, pp. 4185-92, Sep 1 2000.

[6]G. L. Cote, "Noninvasive and minimally-invasive optical monitoring technologies," J Nutr, vol. 131, pp. 1596S-604S, May 2001.

[7]" http://www.coolnurse.com/tattoo.htm."

[8]M. J. McShane, "Potential for glucose monitoring with nanoengineered fluorescent biosensors," Diabetes Technol Ther, vol. 4, pp. 533-8, 2002.

[9]R. Ballerstadt, A. Gowda, and R. McNichols, "Fluorescence resonance energy transfer-based near-infrared fluorescence sensor for glucose monitoring," Diabetes Technol Ther, vol. 6, pp. 191-200, Apr 2004.

[10] P. S. Grant and M. J. McShane, "Development of multilayer fluorescent thin film chemical sensors using electrostatic self-assembly," IEEE Sensors Journal, vol. 3, p. 139, 2003.

[11] S. Chinnayelka and M. J. McShane, "Microcapsule biosensors using competitive binding resonance energy transfer assays based on apoenzymes," Anal Chem, vol. 77, pp. 5501-11, Sep 1 2005.

[12] S. Chinnayelka and M. J. McShane, "Glucose-sensitive nanoassemblies comprising affinity-binding complexes trapped in fuzzy microshells," J Fluoresc, vol. 14, pp. 585-95, Sep 2004.

[13] M. J. McShane, "Microcapsule Glucose Sensors: Engineering systems with enzymes and glucose-binding sensing elements," in Topics in Fluorescence. vol. 10, J. R. Lakowicz and C. D. Geddes, Eds., 2006.

[14] H. Zeng, C. MacAulay, D. I. McLean, and B. Palcic, "Reconstruction of in vivo skin autofluorescence spectrum from microscopic properties by Monte Carlo simulation," J Photochem Photobiol B, vol. 38, pp. 234-40, Apr 1997.

[15] S. L. Jacques and M. Keijzer, "Dosimetry for lasers and light in dermatology: Monte Carlo simulations of 577 nm-pulsed laser penetration into cutaneous vessels." vol. 1422: SPIE, 1991, pp. 2-13.

[16] M. J. C. Vangemert, S. L. Jacques, H. J. C. M. Sterenborg, and W. M. Star, "Skin Optics," Ieee Transactions on Biomedical Engineering, vol. 36, pp. 1146-1154, Dec 1989.

[17] S. L. Jacques, S. Rastegar, M. Motamedi, S. L. Thomsen, J. Schwartz, J. Torres, and I. Mannonen, "Liver photocoagulation with diode laser (805nm) vs. Nd: YAG laser (1064nm)," SPIE Proc., 1992.

[18] E. W. Stein, S. Singh, and M. J. McShane, "Microscale enzymatic optical Biosensors using mass transport limiting hanofilms. 2. Response modulation by varying analyte transport properties," Analytical Chemistry, vol. 80, pp. 1408-1417, Mar 1 2008.

[19] M. Lualdi, A. Colombo, B. Farina, S. Tomatis, and R. Marchesini, "A phantom with tissue-like optical properties in the visible and near infrared for use in photomedicine," Lasers in Surgery and Medicine, vol. 28, pp. 237-243, 2001.

[20] F. P. Bolin, L. E. Preuss, R. C. Taylor, and R. J. Ference, "Refractive-Index of Some Mammalian-Tissues Using a Fiber Optic Cladding Method," Applied Optics, vol. 28, pp. 2297-2303, Jun 15 1989.

[21] "http://omlc.ogi.edu/software/iad/index.html."

[22] S. A. Prahl, M. J. C. Vangemert, and A. J. Welch, "Determining the Optical-Properties of Turbid Media by Using the Adding-Doubling Method," Applied Optics, vol. 32, pp. 559-568, Feb 1 1993.

[23] "http://omlc.ogi.edu/calc/mie_calc.html."